Chapter 5
Impact of Injection Style on the Evolution of Fluid-Induced Seismicity and Permeability in Rock Mass at 410 m Depth in Äspö Hard Rock Laboratory, Sweden

Arno Zang, Ove Stephansson, and Günter Zimmermann

Abstract An underground experiment in Äspö Hard Rock Laboratory is described to bridge the gap between findings from laboratory hydraulic fracturing tests and wellbore-size fluid stimulation in hard rock. Three different water injection schemes are tested quantifying seismic radiated energy, hydraulic energy pumped into the rock, and resulting permeability of the generated fractures. Six hydraulic fracturing tests are performed from a horizontal borehole 102 mm in diameter and 28 m long at 410 m depth and drilled from an existing tunnel in the direction of minimum horizontal stress. Fracture initiation and propagation are mapped by acoustic emission monitoring and impression packer in a rock mass volume $30 \times 30 \times 30$ m in size. In tendency, the fracture breakdown pressure is lower and the number of fluid induced seismicity events is smaller if conventional monotonic hydraulic fracturing is replaced by cyclic, progressive injection and/or pulse pumping schemes. The related permeability of the generated fracture can be increased. The maximum permeability increase results from a combination of cyclic and pulse hydraulic fracturing. Laboratory testing of drill-cores from the long borehole show that dynamic pulsing in combination with progressive cyclic pressurization lower fracture breakdown pressure 10–20%. The interpretation for this result is that during fatigue hydraulic fracturing by cyclic/pulse pumping, a larger process zone develops which is accompanied by many smaller seismic events.

Ove Stephansson died before publication of this work was completed.

A. Zang (✉) · O. Stephansson
Section 2.6 Seismic Hazard and Risk Dynamics, German Research Center for Geosciences GFZ, Potsdam, Germany
e-mail: zang@gfz-potsdam.de

G. Zimmermann
Section 4.8 Geoenergy, German Research Center for Geosciences GFZ, Potsdam, Germany
e-mail: zimm@gfz-potsdam.de

5.1 Introduction

The recent grow in energy technologies like shale gas and geothermal, as well as the
management of subsurface gas reservoirs has led to increased human interaction
with rocks in the Earth's crust. The key ingredient in the discussion of extraction and
storage of energy are subsurface fracture systems, their geometry and stability. The
instability of fractures is documented in induced seismicity monitored close to the
operation sites. This is because human activity perturbs subsurface stresses by fluid-
injection or depletion induced by pore pressure changes, causing fractures to grow,
coalesce and slip. A classification of fluid-induced seismicity has been suggested
e.g. by Ellsworth (2013) and McGarr et al. (2015) though the seismic radiated energy
is only a small fraction of the pumped-in hydraulic energy (e.g. in the hydraulic
fracture grow process), injection activities are terminated as a result of the felt
induced seismicity, e.g. in geothermal operations Giardini (2009). Zang et al.
(2014) give an overview of induced seismicity related to geothermal operations
and Grünthal (2014), in particular, analyzes the occurrence of seismic events of
economic concern. At a specific site the task is to detect, image and control fractures
for mechanical and hydraulic integrity of the reservoir under investigation.

As field tests in wellbores are time consuming and costly, we see controlled
experiments in underground research facilities and mines as a valuable alternative to
seek for optimum energy extraction methods with advanced fluid-injection schemes.
The optimization process can involve fracture design with minimum seismic radi-
ated energy and/or fracture design with maximum permeability enhancement. For
this, radiated seismic energy and pumped-in hydraulic energy needs to be quantified
for various injection schemes applied to target rock in well-known stress conditions.

5.2 Underground Experiment in Granitic Rock

The Äspö Hard Rock Laboratory (HRL) is located in the southeastern part of
Sweden about 30 km north of the city of Oskarshamn. It has been selected to fix
relevant variables for performing controlled fluid injection experiments. In the first
place, the stress state at 410 m depth is fixed, and well known from hydraulic
fracturing by Klee and Rummel (2002) and overcoring stress measurements by
Ask (2006). Second, the granitic rock types are fixed, and relevant for geothermal
reservoir development. Äspö granodiorite, gabbro and fine-gained granite are well
characterized, both mechanically and hydraulically. Third, the total volume of fluid
injected is limited to 30 liters maximum. This allows investigating the impact of
injection style on seismic radiated and hydraulic energy in naturally fractured
granitic rock mass with size of about 30 × 30 × 30 m, see Fig. 5.1 after Zang

Fig. 5.1 Hydraulic fracture design and high-frequency sensor array at 410 m depth in Äspö HRL. (**a**) Map view of horizontal fracturing borehole F1 drilled in the orientation of minimum horizontal stress. Monitoring boreholes (M1–M3) are equipped with AE sensors. Short holes in the tunnel roof are equipped with both AE sensors and accelerometers. (**b**) Installing a chain of AE sensors in tunnel TASN
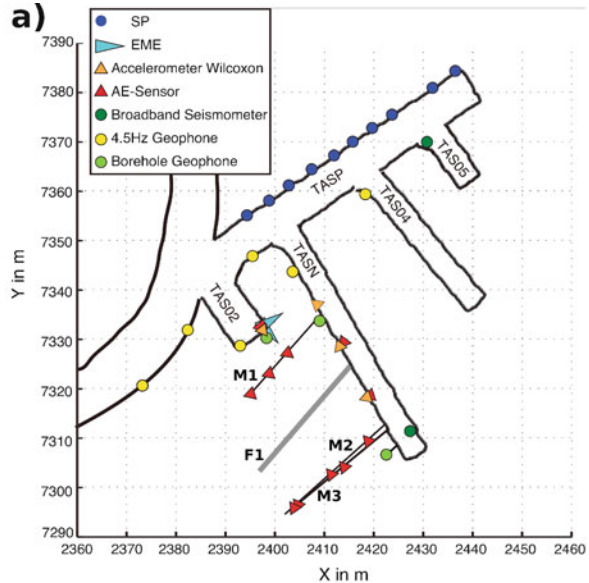
et al. (2017). Six borehole intervals free of visible fractures are identified for hydraulic testing. Three different water-injection schemes are applied (Fig. 5.2).

Conventional hydraulic fracturing (HF) with continuous fluid injection follow the ISRM suggested method for hydraulic fracturing stress measurements Haimson and Cornet (2003). The typical test starts with the initiation of the packer system to seal the interval, followed by a rapid pressurization with water to test the system for potential leakage (pulse integrity test). During the subsequent main test phase a constant injection rate is applied (see Fig. 5.2a). Pressure increases until it reaches the fracture breakdown pressure (FBP), followed by a decline to a stable pressure level called the fracture propagation pressure. After stable pressure conditions are reached, the well is shut-in and the pressure drops rapidly to the instantaneous shut-in pressure (ISIP) followed by a decline curve. The ISIP is assumed to be equivalent to the minimum principal stress. Finally, the interval pressure is released and the

Fig. 5.2 Schematics of the three hydraulic testing methods applied in the horizontal borehole at 410 m depth in Äspö HRL; (**a**) conventional test with constant flow rate, (**b**) progressively increasing flow rate with cyclic flow rate, and (**c**) progressively increasing and pulsed cyclic flow rate. (Modified from Zimmermann et al. 2019)

conventional test with constant flow rate

progressively increasing flow rate

progressively increasing and pulsed flow rate

pressure pulses
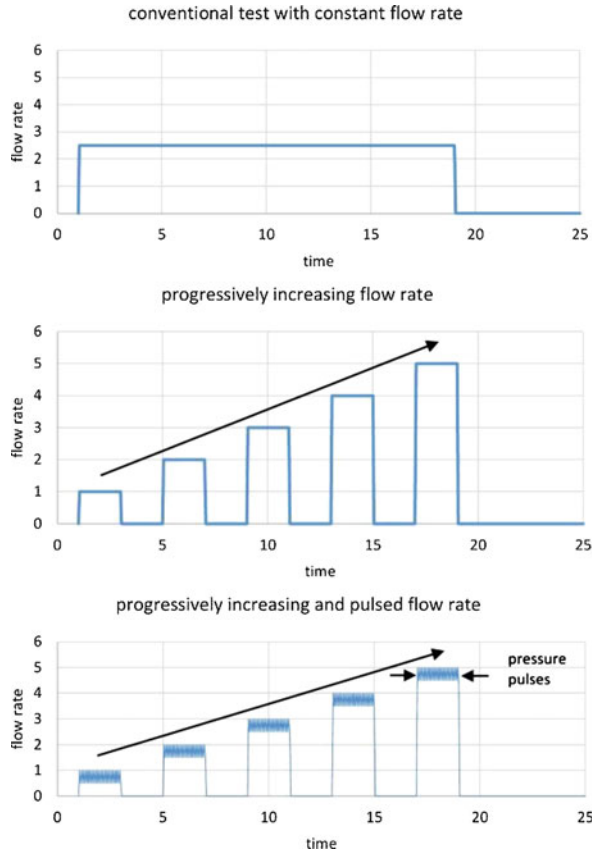
fluid volume is recovered. The test procedure is repeated several times to obtain the fracture reopening pressure (FRP) at each test cycle. The tensile strength of rock is calculated from FBP-FRP. It is assumed that the fracture has been closed completely in between the cycles. The test procedure for the progressive water injection consists of a modified pressure scheme. First the pressure is increased to 20% of FBP obtained from the conventional test in the same formation. Then, a shut-in for several minutes follows with subsequent pressure release (phase of depressurization). Then, the pressure is increased by a level ca. 10% above the previous pressure level following the same scheme. After shut-in another depressurization phase follows. Sequences of pressurization and depressurization alternate until a pressure drop indicates rock failure. This treatment is best described as a cyclic hydraulic pressure scheme with progressively increasing flow rate, see Fig. 5.2b. The subsequent re-fracturing stages follow the same scheme like in the conventional test. The treatments differ only for pressures below the FBP, i.e. single-flow rate tests are replaced by multiple-flow rate fracture breakdown tests.

The fatigue hydraulic fracturing (FHF) test procedure is a combination of the progressive injection test and a pulse hydraulic fracturing (PHF) test. The hydraulic

equipment for the pulse dynamic test consists of a hydraulic pump to maintain linear and dynamic pressure levels (pressurization bands) together with a second hydraulic pressure pump to drive the dynamic pulse tool with adjustable amplitude and frequency (5–20 Hz). Both pressure signals are combined to result in dynamic pressure pulses on different predefined hydraulic pressure levels based on the FBP of conventional tests carried out previously. The FHF test is best described as a test with cyclic increasing target pressure and additional high frequency pressure oscillations in pressurization phases with step-wise increasing target pressure and flow rate, see Fig. 5.2c. Also this test procedure is frequently interrupted by depressurization phases where crack tip stresses are released.

The in situ testing of different injection schemes with monitoring associated seismic and electro-magnetic signals is conducted in the horizontal borehole F1, 102 mm in diameter and 28 m long, drilled from tunnel TASN in the direction of minimum horizontal stress (Fig. 5.1a). Fluid-induced hydraulic fractures open and propagate in radial planes following the on-site in situ stress conditions ($S_V=S_H > S_h$). The high frequency seismic network used consists of 11 acoustic emission (AE) sensors (Fig. 5.1a, red triangles, frequency 1–100 kHz) and four accelerometers (Fig. 5.1a, orange triangles, frequency below 25 kHz). AE sensors are implemented in three monitoring boreholes located left and right of the hydraulic testing borehole (Fig. 5.1a, M1–M3). In Fig. 5.1b, the borehole implementation of a chain of AE sensors is shown. The remaining AE sensors and accelerometers are implemented in short boreholes in the roof of the surrounding tunnels. This monitoring design allows following hydraulic fracture nucleation and growth since the fracture opens perpendicular to the minimum principal stress S_h, and rapidly grows in the plane containing the intermediate S_H and maximum principal stress SV, which is the direction towards the monitoring boreholes (Zang et al. 2017).

A continuous and a triggered recording system are in operation at 1 MHz sampling rate. This allows near real-time tracking of the hydraulic fracture growth process Kwiatek et al. (2017), and post processing of full waveforms Lopez Comino et al. (2017) for source analysis. From a seismological point of view, full waveforms recorded during injection tests have excellent data quality for further processing which includes hypocenter locations, relocations, and in depth investigations of fracture source, growth and coalescence.

5.3   Results

In this section, the seismic response of the high-frequency sensor network from six hydraulic tests in the horizontal borehole at 410 m depth is presented with the permeability enhancement process inferred from hydraulic data, and the fracture pattern inferred from impression packer test results. Laboratory tests with cyclic increasing target pressure and additional high frequency pressure oscillations in pressurization phases with step-wise increasing target pressure were conducted on

90 mm drill-cores taken at the location of the six test intervals in the horizontal borehole F1.

5.3.1 Seismic Radiated Energy

In Fig. 5.3, hydraulic test parameters like FBP, FRP, flow rate and injected volume are compared with the total number of AE events localized (color bars) for different rock types and injection schemes. In the deeper section of the horizontal borehole, F1 three hydraulic tests are carried out in Ävrö granodiorite, two conventional continuous injection tests and one progressive cyclic injection test. Compared to the conventional tests (HF1, HF2), the AE activity in the progressive test (HF3) starts at a later stage of the treatment, and the total number of seismic events is less. Experiment HF3 reveals a FBP of approximately 9.2 MPa. The conventional test with continuous water injection in the same rock type (HF2), leads to a value of FBP 15% larger than compared to the cyclic, progressive test. The two tests in diorite
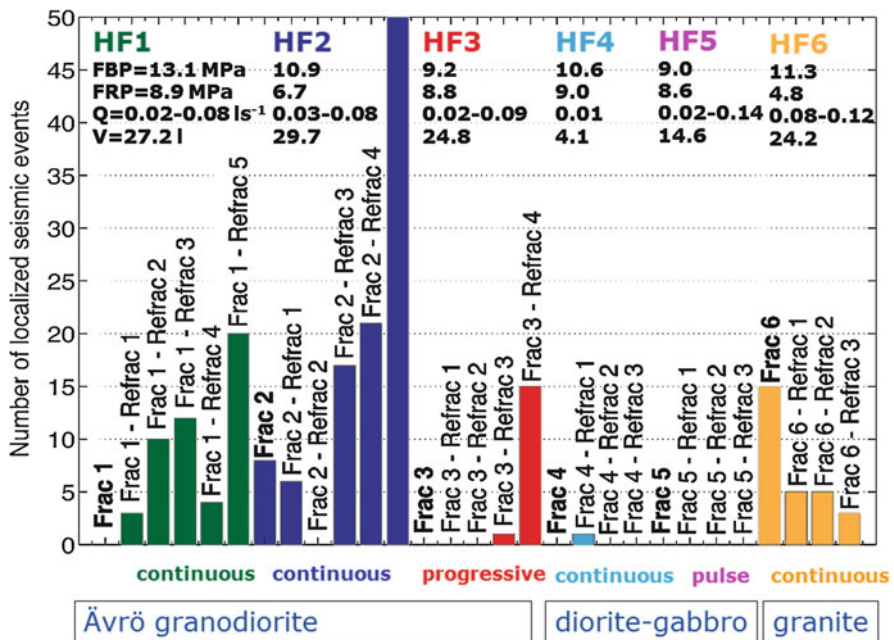

Fig. 5.3 Number of localized seismic events is shown per fracturing stage for six hydraulic tests in horizontal borehole F1 at 410 m depth in Äspö HRL. In each experiment, the fracture breakdown pressure, fracture reopening pressure, flow rate range, and total volume of water injected is listed. The first test, HF1 starts in the deeper part of the 28 m long, horizontal borehole (25 m), and the last test HF6, is operated about 5 m from the onset of F1 at the tunnel wall

gabbro generated only one AE event indicating that this rock type is less seismic active than the Ävrö granodiorite when monitored with the same trigger level.

In test HF5, the progressive pulse testing is applied mimicking the FHF treatment with the high frequency oscillation pressure generated by the dual pump system. This test results in a lower FBP (9.0 MPa) compared to the conventional test in the same rock HF4 (FBP = 10.6 MPa), see Fig. 5.3.

In the fine-grained granite close to the tunnel wall (HF6), seismic activity is observed in all fracturing stages. In contrast to other tests, in the granite the maximum number of seismic events occurred during early stages of the hydraulic fracturing and re-fracturing experiment, Fig. 5.3.

In Fig. 5.4, the evolution of acoustic emission events over time is shown for neighboring test intervals (HF2 and HF3) with different injection schemes in the same rock, Ävrö granodiorite. For this, the hydraulic data (injection pressure and flow rate) are plotted together with the AE activity. In Fig. 5.4a, the conventional HF test HF2 and in Fig. 5.4b, the progressive cyclic test scheme H3F is shown for a full sequence of fracturing and re-fracturing stages. While AE events are observed during all fracturing stages (except refrac2) of the conventional test HF2 (Fig. 5.4a), in experiment HF3 with cyclic progressive water injection, AE events occur in the third and fourth re-frac stage, only (Fig. 5.4b). No AE occur before the FBP in the second last cyclic, progressive treatment in test HF3 despite the steady increase of flow rate for the last three cycles.

5.3.2   Permeability Enhancement Process

In Fig. 5.5, the permeability enhancement process in Ävrö granodiorite is compared for the two schemes HF2 and HF3 displayed in Fig. 5.4. The permeability is estimated from the hydraulic pressure decay curves, Zimmermann et al. (2019). The initial permeability of rock is estimated from the first data point in the test, e.g. 0.1 mD (Fig. 5.5, HF2). In this test, the increase in permeability is 1.3 mD after the initial fracturing and 4.8 mD after the last refrac stage. In the same period of time, eight AE are registered before the FBP, and totally 102 AE at the end of the experiment.

In the cyclic progressive test HF3, seismicity is observed in the last two re-fracturing stages, only (Fig. 5.4b). The permeability, however, increases mono-tonically in cyclic treatment from 0.2 mD before FBP to 2 mD after the last re-fracturing cycle (refrac4), see Fig. 5.5.

This demonstrates that the injection style has a strong impact on both, the total number of seismic events observed (conventional 102, cyclic progressive 16), and the maximum magnitude of the AE events (conventional 49 dB, cyclic progressive 43 dB). The permeability enhancement process shows a higher permeability for conventional HF 5.0 mD and less for cyclic progressive treatment, 2 mD. Note that the rock permeability may increase while the associated fracturing mechanisms are below the AE detection limit. The maximum permeability performance was reached
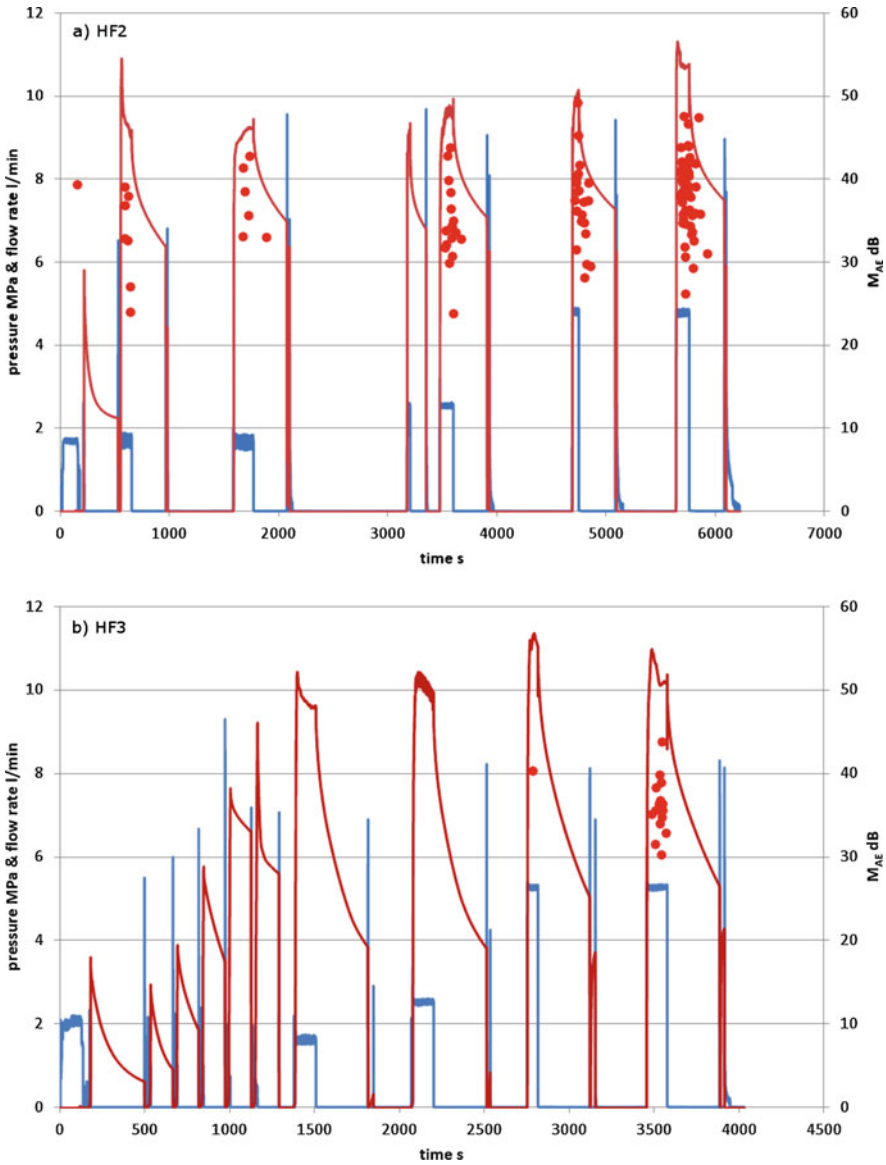
Fig. 5.4 Injection pressure and flow rate (left axis, red and blue) and AE magnitude (right axis, red dots) versus time for hydraulic fractures generated with two different injection schemes: (**a**) conventional hydraulic fracturing HF2, and (**b**) cyclic, progressive injection scheme HF3 – one method to mimick fatigue hydraulic fracturing. (Modified after Zang et al. (2017)

Fig. 5.5 Permeability inferred from pressure decay curves in Ävrö granodiorite for neighboring test intervals with two different water-injection schemes versus time: conventional hydraulic fracturing HF2, and cyclic, progressive injection scheme in experiment HF3. (Modified after Zimmermann et al. 2019)
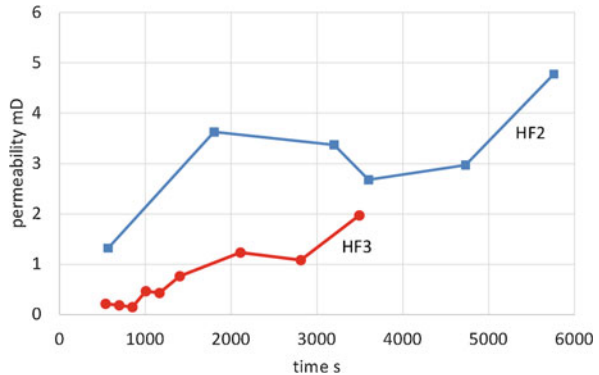
by progressive pulse testing (Fig. 5.2c). However, no acoustic emissions could be detected in the corresponding rock type, diorite gabbro.

5.3.3 Fracture Pattern from Impression Packer

When comparing the orientation of hydraulic fractures in Ävrö granodiorite we find from impression packer results a single fracture plane in conventional testing (HF2), and we find two fracture planes in the cyclic, progressive test HF3. This finding is in line with results from the AE hypocenter distributions which indicate a single fracture plane for tests HF2 while in test HF3, a more complex fracture pattern is evident, see Fig. 5.6.

The fracturing test HF5 was performed as a dynamic pulse test with progressively increasing flow rate and pressure pulse on top. The test was carried out at a borehole depth of 13.3 m in fine grained diorite-gabbro. During the whole HF5 test no AE events was recorded while permeability increased from 2.3 mD to more than 25 mD. The minor fracture trace recorded from the impression packer is shown in Fig. 5.6.

The strike direction and dip angle of the recorded fractures from the impression packer tests and the orientation of the major S_1, intermediate S_2 and minor principal stress S_3 from overcoring stress measurements conducted by Ask (2006) are presented in Fig. 5.7. The majority of induced hydraulic fractures are aligned with the direction of the maximum principal stress and dipping in average 70 degrees in the direction of the intermediate principal stress.

Kwiatek et al. (2018) investigated the source characteristics of picoseismicity recorded during the six hydraulic fracturing in situ experiments, HF1-HF6. The combined seismic network allowed for detection and detailed analysis of 196 small scale seismic events with moment magnitudes $M_w < -3.5$ that occurred during the stimulations and shortly after, see Fig. 5.8.
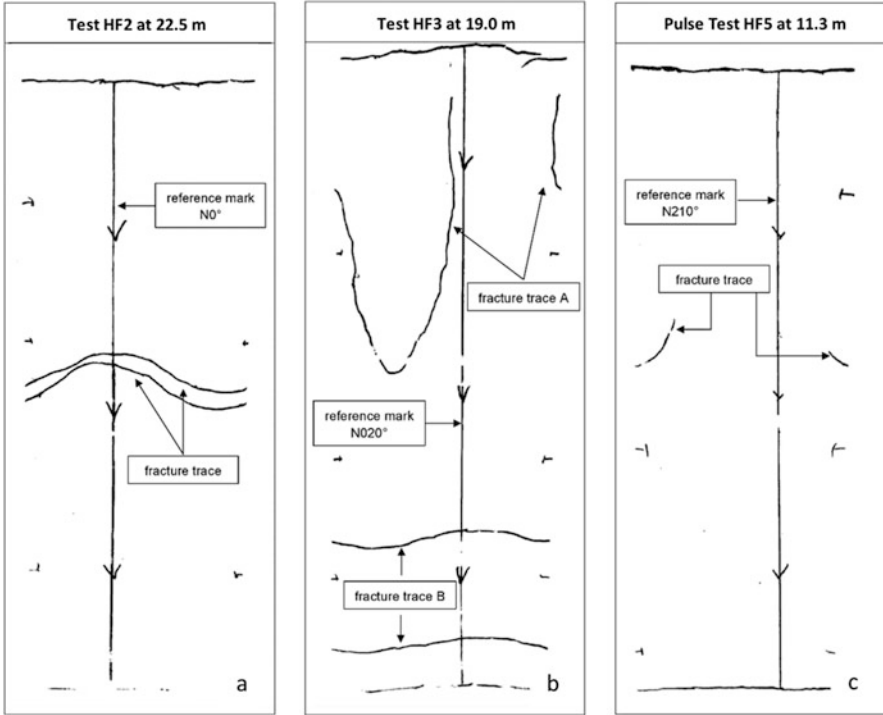
Fig. 5.6 Impression packer test images of hydraulic fracturing experiments in borehole F1; (**a**) HF2 at 22,5 m depth in Ävrö granodiorite; (**b**) HF 3 at 19.0 m depth in Ävrö granodiorite and (**c**) HF5 at 11.3 m in diorite gabbro. (After Zimmermann et al. 2019)

5.4   Discussion

At mine scale with decameter size hydraulic fractures, FBP in Ävrö granodiorite is lowered by 15% when using neighboring injection intervals, and replacing mono-tonic (10.9 MPa) by cyclic, progressive water injection (9.2 MPa). The total number of AE located is reduced from 102 events (HF2, monotonic injection) to 16 AE events (HF3, cyclic progressive injection). The combination of cyclic and pulse hydraulic fracturing (HF5) resulted in zero AE but in a different rock type (diorite gabbro). Compared to the initial value of permeability in the conventional hydraulic fracturing test HF2, the permeability increases by 3.5 mD compared to 1.8 mD in the cyclic progressive injection case HF3. The trend of permeability increase is less advanced for the cyclic injection scheme compared to the conventional test, but also leads to lower seismicity. In case further experiments confirm these findings, it can be concluded that, to achieve a similar permeability increase, a cyclic treatment needs to have a longer duration and hence will be more costly. With respect to field applications, it seems to be a feasible option to reduce the risk of unwanted seismic

Fig. 5.7 Fracture location and orientation from impression packer of all tests in borehole F1. The strike of majority of generated fractures agrees with the azimuth of the maximum principal stress S1 and the dip is sub-parallel with the dip and dip direction of the least principal stress S3 from overcoring data
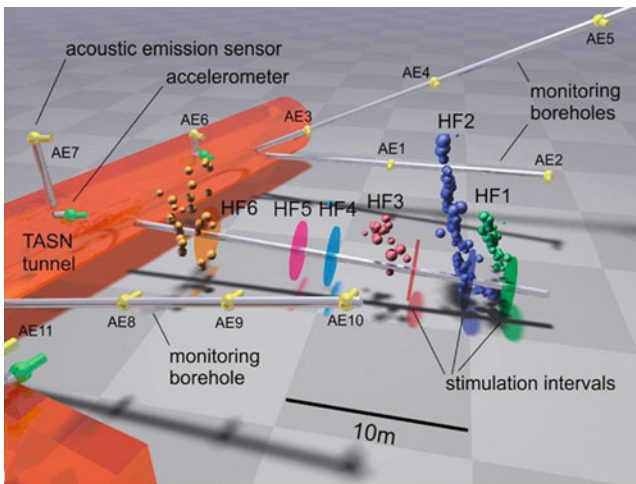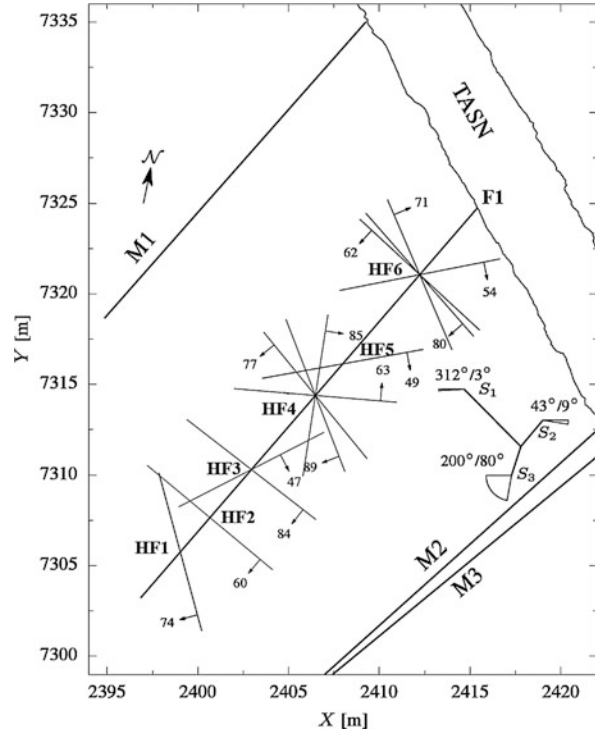

Fig. 5.8 Spatial view of rock mass from NW. The seismic activity is shown with spheres reflecting the stimulation stage and size corresponding to the moment magnitude. Colored disks reflect the stimulation intervals in borehole F1. From borehole bottom to the onset: green (HF1); blue (HF2); red (HF3); teal (HF4); magenta (HF5) and yellow (HF6). Yellow and green bottle-shaped objects are AE sensors and accelerometers. (After Kwiatek et al. 2018)

events and hence foster the public acceptance. In addition, the fracture from impression packer indicates a single fracture plane in conventional tests (HF1).

We see acoustic emission events as a result of originating from process zone related micro-shears in Ävrö granodiorite while we agree with Warpinski et al. (2012) that the amount of energy radiated as elastic waves is only a small fraction of the injection energy of the pump.

Stephansson et al. (2019) performed laboratory pulse tests in combination with cyclic increasing pressurization on cores from the test intervals of the hydraulic fracturing borehole F1 at Äspö HRL. Two cores from each of the three different rock types are tested and after each cycle a 3-min-long dynamic pressure pulses of amplitude 4 MPa and frequency 1 Hz are superimposed at each progressive cycle with constant pressure. The majority of the laboratory tests of different rock types at Äspö HRL show that dynamic pulsing in combination with progressive cyclic pressurization reduces the breakdown pressure of the order of 10–20% for the fine-grained granite and diorite-gabbro, respectively. No reduction in breakdown pressure from cyclic pressurization and dynamic pulsing is observed for the two core samples of Ävrö granodiorite. The most likely explanation for the lack of reduction is the mineral composition and degree of metamorphose of the granodiorite and a higher hydraulic strength of the sample tested with cyclic increasing pressure and pulses.

We see the larger fracture process zone with more complex fracture pattern evolving during cyclic progressive and pulse hydraulic fracturing as a result of frequent changes of the fracture direction caused by depressurization phases and stress relaxation at the fracture tip. Stress changes can be explained by (a) pore pressure increase due to freshly created fractures in the process zone, and by (b) rock chips removed from fracture faces by oscillations during fatigue hydraulic fracturing. As a consequence, larger seismic events in conventional hydraulic fracturing are mitigated by smaller seismic events caused by arresting and branching fractures during the fatigue treatment. In terms of energy balance, less fracture energy is needed and less seismic energy is radiated, if a hydraulic fracture runs through a rock volume which is efficiently fragmented beforehand.

5.5   Conclusion

In this study, advanced fluid injection schemes are tested in well controlled rock and stress conditions at mine scale and in the laboratory. At mine scale, the horizontal borehole for fluid injection at 410 m depth in Äspö HRL has a diameter of 102 mm and a total length of 28 m. Hydraulic tests in naturally fractured granite with maximum 30 liter of water injected generated small-scale hydraulic fractures with extension ca. 20–30 square meter. The seismic response of the hydraulic fracture strongly depends on injection style and rock type. In the same rock, cyclic, progressive injection and pulse injection produced less acoustic emission activity as compared to conventional, continuous fluid-injection. Also, the fracture pattern inferred

from impression packer results and acoustic emission hypocenter solutions turns out to be more complex when replacing conventional by fatigue hydraulic fracturing. We see the larger fracture process zone with more complex fracture pattern evolving during cyclic progressive and pulse hydraulic fracturing as a result of depressurization phases and stress relaxation at the fracture tip. This conclusion applies to laboratory and mine scale tests. As a consequence, larger seismic events in conventional hydraulic fracturing are mitigated by smaller seismic events caused by arresting and branching fractures during the fatigue treatment.

References

Ask D (2006) Measurement-related uncertainties in overcoring data at the Äspö HRL, Sweden. Part 2: Biaxial tests of CSIRO HI overcore samples. Int J Rock Mech Min Sci 43(1):127–138

Ellsworth WL (2013) Injection-induced earthquakes. Science 341:1225942. https://doi.org/10.1126/science.1225942

Giardini D (2009) Geothermal quake risk must be faced. Nature 426:848–849

Grünthal G (2014) Induced seismicity related to geothermal projects versus natural tectonic earthquakes and other types of induced seismicity events in Central Europe. Geothermics 52:22–35

Haimson BC, Cornet F (2003) ISRM suggested methods for rock stress estimation-part 3: hydraulic fracturing (HF) and/or hydraulic testing of pre-existing fractures (HTPF). Int J Rock Mech Min Sci 40(7–8):1011–1020

Klee G, Rummel F (2002) Rock stress measurements at the Äspö HRL Hydraulic fracturing in boreholes, Technical Report IPR-02-02. Stockholm, SKB

Kwiatek G, Plenkers K, Martinez Garzon P, Leonhardt M, Zang A, Dresen G (2017) New insights into fracture process through in-situ acoustic emission monitoring during fatigue hydraulic fracture experiment in Äspö Hard Rock Laboratory. Proc Eng 191:618–622

Kwiatek G, Martínez-Garzón P, Plenkers K, Leonhardt M, Zang A, von Specht S et al (2018) Insights into complex sub-decimeter fracturing processes occurring during a water injection experiment at depth in Äspö Hard Rock Laboratory, Sweden. J Geophys Res Solid Earth 123:6616–6635

Lopez Comino J, Heimann S, Cesca S, Grigoli F, Milkereit C, Dahm T, Zang A (2017) Characterization of hydraulic fractures growth during the Äspö Hard Rock Laboratory Experiment (Sweden). Rock Mech Rock Eng 50:2985–3001

McGarr A, Bekins B, Burkardt N, Dewey J, Earle P, Ellsworth W, Ge S, Hickman S, Holland A, Majer E, Rubinstein J, Sheehan A (2015) Coping with earthquakes induced by fluid injection. Science 347(6224):830–831

Stephansson O, Semikova H, Zimmermann G, Zang A (2019) Laboratory pulse test of hydraulic fracturing on granitic sample cores from Äspö HRL, Sweden. Rock Mech Rock Eng 52:629–633

Warpinski NR, Du J, Zimmer U (2012) Measurements of hydraulic-fracture-induced seismicity in gas shales. SPE Prod Op 27:240–252

Zang A, Oye V, Jousset P, Deichmann N, Gritto R, McGarr A, Majer E, Bruhn D (2014) Analysis of induced seismicity in geothermal reservoirs – an overview. Geothermics 52:6–21

Zang A, Stephansson O, Stenberg L, Plenkers K, Specht S, Milkereit C, Schill E, Kwiatek G, Dresen G, Zimmermann G, Dahm T, Weber M (2017) Hydraulic fracture monitoring in hard rock at 410 m depth with an advanced fluid-injection protocol and extensive sensor array. Geophys J Int 208(2):790–813

Zimmermann G, Zang A, Stephansson O, Klee G, Semikova H (2019) Permeability enhancement and fracture development of hydraulic fracturing experiments in the Äspö Hard Rock Laboratory, Sweden. Rock Mech Rock Eng 52:495–515